Molecular laser stabilization at low frequencies for the LISA mission

B. Argence, H. Halloin, O. Jeannin, P. Prat, O. Turazza, E. de Vismes, G. Auger, and E. Plagnol
APC, Université Paris 7 Denis Diderot, 10, rue Alice Domon et Léonie Duquet, 75205 Paris Cedex 13, France
(Received 14 January 2010; published 27 April 2010)

We have developed a 532 nm iodine stabilized laser system that may be suitable for the LISA mission (Laser Interferometer Space Antenna) or other future spaceborne missions. This system is based on an externally frequency-doubled Nd:YAG laser source and uses the molecular transfer spectroscopy technique for the frequency stabilization. This technique has been optimized for LISA: compactness (less than 1.1×1.1 m^2), vacuum compatibility, ease of use and initialization, minimization of the number of active components (acousto-optic modulators are both used for frequency shifting and phase modulating the pump beam). By locking on the a_{10} hyperfine component of the R(56)32-0 transition, we find an Allan standard deviation (σ) of 3×10^{-14} at 1 s and $\sigma < 2 \times 10^{-14}$ for 20 s $\leq \tau \leq 10^3$ s. In terms of linear spectral density, this roughly corresponds to a stability better than 30 Hz/$\sqrt{\text{Hz}}$ between 10^{-2} and 1 Hz with a stability decrease close to $1/f$ below 10 mHz.

DOI: 10.1103/PhysRevD.81.082002 PACS numbers: 95.55.Sh, 42.62.Eh, 95.55.Ym

I. INTRODUCTION

The Laser Interferometer Space Antenna (LISA) mission is a joint spaceborne project of the European Space Agency and the National Aeronautics and Space Administration (ESA-NASA), aiming at detecting gravitational waves in the frequency range 10^{-4}–1 Hz [1]. It consists of three spacecraft in a nearly equilateral configuration orbiting around the Sun, about 20 degrees behind the Earth. The spacecrafts are separated by 5×10^6 km, constantly following free-flying masses located at their center.

On each spacecraft, two laser beams are emitted toward the other satellites, resulting in six laser links. These interferometric measurements are used to precisely monitor the distance between the inertial masses and, hence, to detect the tiny variation due to the passage of a gravitational wave. So, the expected performance of LISA relies on two main technical challenges: the ability for the spacecrafts to precisely follow the free-flying masses and an outstanding precision of the phase shift measurement.

The goal of LISA is to detect gravitational deformations as small as $\Delta L/L \approx 7 \times 10^{-21}/\sqrt{\text{Hz}}$ (i.e., 7 pm per million of km) around 5 mHz. Contrary to a classical Michelson interferometer, the optical signal is obtained from two different laser sources. As a consequence the beam phase noise does not vanish and the relative frequency stability of the lasers must be at the same level as the expected sensitivity ($\Delta L/L = \Delta\nu/\nu$). This requirement is far beyond any standard stabilization technique developed on ground and foreseeable for a future space mission.

Nevertheless, this stability can be achieved for LISA thanks to three successive stabilization stages:

(i) *Time delay interferometry* (TDI) [2]: While each optical signal is the combination of two laser sources, the frequency noise of each source is also propagating on two laser links. Thus, by correctly combining the interferometric signals, taking into account the propagation delays (around 16 s between two spacecrafts), it is possible to cancel the laser noises (and, so, recover a ''Michelson-like'' signal). However, due to the finite precision of the time stamps (drifts of the ultra stable clocks), the application of this method is not perfect and the noise reduction factor is of the order of 10^8.

(ii) *Arm-locking* [3–5]: In the interesting frequency range of LISA (10^{-4}–1 Hz), the distance between the free-falling masses is very stable. Consequently, it can be used as a length (i.e., frequency) reference. This technique requires the frequency reference of the prestabilization to be slightly tunable.

(iii) *Prestabilization*: Even with TDI and arm-locking, the light emitted by the laser sources needs to be very stable, at the level of 10^{-13} in terms of relative frequency change. Up to now, prestabilization on a Fabry-Perot cavity has been considered [6]. However, another prestabilization technique often used in metrology [7–9], based on the use of a hyperfine transition of the iodine molecule as frequency discriminator, may be an interesting way.

II. PRESTABILIZATION TECHNIQUES FOR LISA

The Fabry-Perot (FP) prestabilization technique is based on a fixed-length, ultra stable optical resonator. It was proved to meet the LISA requirement in terms of intrinsic frequency stability [6] by means of the well-known Pound-Drever-Hall stabilization method. Its tunability has been recently demonstrated using an additional electro-optic modulator and sideband locking [10].

Nevertheless, some limitations can be identified with this technique. First, the performance of the FP cavity is very sensitive to mechanical but mainly thermal disturbance. For example, the thermal stability of the tanks housing the cavities must be of the order of 10 μK/$\sqrt{\text{Hz}}$ at 1 mHz. Over very long time ranges (days), they can even

exhibit frequency drifts of many megahertz [11,12]. Additionally, they do not provide an absolute frequency reference. When two lasers are stabilized on two independent cavities, the smallest beat note frequency can still be up to half of the free spectral range. Consequently, this beat frequency can be outside of the bandwidth of the photodiode (typically 100 MHz). It will therefore be necessary to scan the frequency of one of the systems to get the correct locking point. Finally, the performance of the arm-locking algorithm can be increased with the precise knowledge of the Doppler frequency shift (consequence of the relative drift of one spacecraft with respect to another one) [13].

The work presented here proposes an interesting alternate technique, based on molecular spectroscopy, that can circumvent these issues. It offers the required performance with very good long-term stability (fixed frequency reference) though the reference can be slightly tuned to account for arm-locking. The knowledge of the Doppler shift is therefore directly measured from the beat frequency. With a reasonably simple setup, the repeatability of the locking frequency has a long-term drift of about a few kilohertz or less. Therefore, a beat frequency well within the detector bandwidth will immediately be obtained while mixing two molecular stabilized lasers. The position of a molecular transition is also much less sensitive to thermal perturbations than a cavity, the constraints being typically relaxed by about 3 orders of magnitudes.

III. EXPERIMENTAL SETUP

Using hyperfine transitions to stabilize a laser is common in metrology (see [14] and references therein). Our experimental setup drew inspiration from the work done at the Observatoire de la Côte d'Azur [15]. This system has to both meet the spatial constraints (simplicity, compactness, minimizing the consumption of energy) and achieve frequency-stability performance comparable to those obtained in metrology.

In order to perform a precise analysis of the frequency stability of our iodine stabilized laser, we decided to build two identical systems allowing frequency comparisons. Indeed, the stability of the systems is determined by the measurement of the joint performance. The experimental setup of one of our systems can be seen in Fig. 1. We use commercial, nonplanar ring oscillator (NPRO) Nd:YAG lasers that produce about 1 W light power at 1064 nm. These Nd:YAG lasers present many advantages: they have a good intrinsic power and frequency stability (some MHz/s) and a relatively good tolerance to optical feedback. The long time-scale fluctuations can be corrected by changing the laser crystal temperature and the short ones by squeezing the YAG crystal. Lasers, with similar characteristics, suitable for the LISA mission have already been investigated [16] and are actually, to our knowledge, in technology readiness level (TRL) 4–6 [17].

Unfortunately, there is no known strong molecular resonance to lock the lasers around 1064 nm. However, iodine provides strong, narrow hyperfine transitions around 532 nm corresponding to the second harmonic of Nd:YAG laser. These transitions have been widely used at the laboratory as frequency or length references [8]. And previous experiments using iodine stabilization for LISA have already been done [15,18], and showed promising results.

The frequency of the laser is then doubled with a single pass through a nonlinear crystal of PP:MgLNO, i.e. a

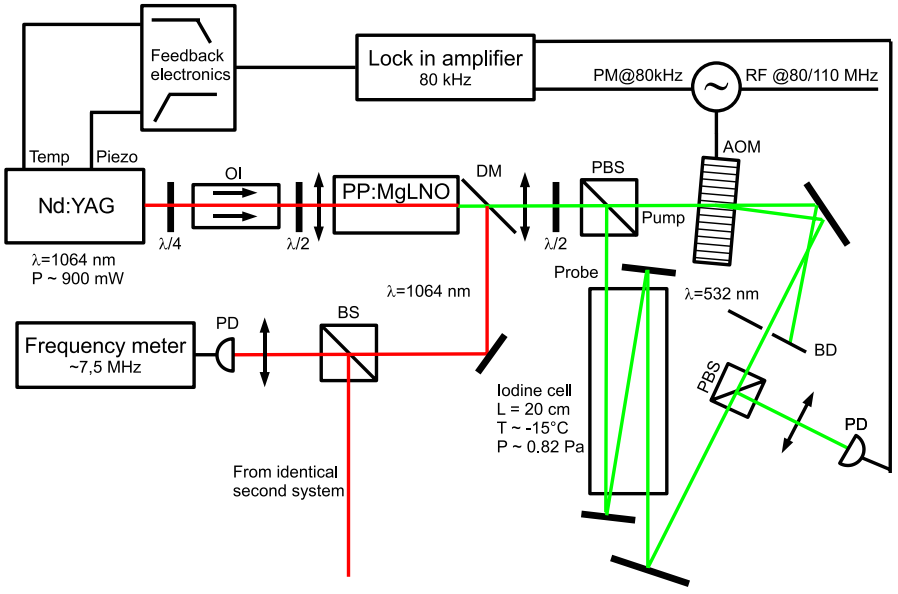

FIG. 1 (color online). Experimental layout of the iodine laser stabilization. OI: optical isolator, DM: dichroic mirror, BS: beam splitter, PBS: polarization beam splitter, AOM: acousto-optic modulator, PD: photodiode, BD: beam dump, PM: phase modulation, and RF: radio frequency.

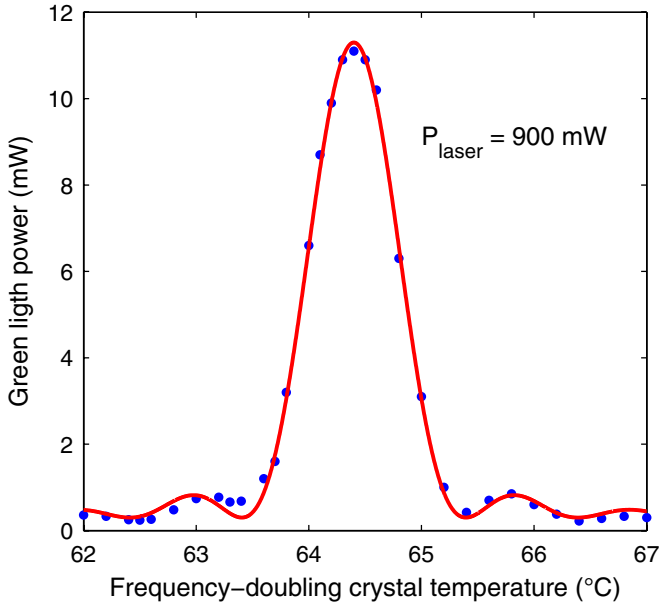

FIG. 2 (color online). Green power evolution versus frequency-doubling crystal temperature. Dots correspond to measured values. Solid curve corresponds to the best fit.

periodically poled crystal of lithium nickel oxide doped by manganese ions. This material had been chosen because of its good efficiency and tolerance to high power density and space radiations [18]. The crystals are parallel-piped; the dimensions are $3 \times 0.5 \times 20$ mm^3.

These crystals are put in an oven and their temperature stabilized at around 65 ± 1 °C (depending on the crystals). Figure 2 shows the output power of green light versus the oven temperature of one of the doubling crystals. Clearly, the frequency-doubling crystal efficiency is really dependent on the crystal temperature. The relation may be fitted by a sinc^2 law:

$$P_{(T)} = a\,\mathrm{sinc}^2[2\pi b(T - c)] + d,$$

where T is the crystal temperature, $P_{(T)}$ the green power, and a, b, c, d parameters:

$a = 11.0 \pm 0.2$ mW (maximum power),

$b = 0.160 \pm 0.004$ °C^{-1} (FWHM$/2\pi$, which is correlated to the crystal length),

$c = 64.40 \pm 0.01$ °C (average temperature), and

$d = 0.3 \pm 0.1$ mW (power offset).

Consequently, electronic developments have been made to stabilize the temperature at a level of 0.01 °C. The temperature of the crystals are then stabilized at $65 \pm 1 \pm 0.01$ °C (1 corresponding to the systematic bias and 0.01 to the 1σ systematic deviation). For an input power of 900 mW, about 11 mW of green light (at 532 nm) is produced. All the input IR power not converted into green light corresponds to the useful beam for LISA.

A dichroic mirror is then used to separate the two wavelengths. The infrared parts of the two systems are then recombined with a beam splitter and sent to a fibered photodiode. The frequency noise of the beat is assumed to be the (quadratic) sum of the frequency noises of each of the systems. The frequency value of the beat is between 7 and 9 MHz, depending on the value of the frequency shifts.

The green beam is divided in two nonequivalent power parts: the pump beam (about 4–5 mW) and the probe beam (0.2–0.3 mW). Both beams counterpropagate within the iodine cell. This configuration allows one to get rid of the Doppler broadening effect due to the thermal movements of the molecules. This technique, called saturation spectroscopy, is commonly used in metrology to lock lasers on an hyperfine (rotovibrational) line [19]. One of these beams (the pump) is strong enough to ''saturate'' the line (i.e., a large part of the molecules on its path are in a excited state). The other beam (the probe), of much weaker intensity, is used to scan the absorption profile. The molecules that have already been excited by the pump beam cannot absorb the probe beam and then cause a dip in the absorption profile. With the two beams being of the same wavelength (or shifted by a constant value, see below), only molecules with a given velocity (projected on the light path) are simultaneously saturated by the pump and scanned by the probe beams.

The pump beam is frequency shifted and frequency modulated by an acousto-optic modulator (AOM). The method used here is modulation transfer spectroscopy (MTS), which already demonstrated very good results on similar experiments [7]. The modulation frequency is at 80 kHz with a frequency shift of about 80 MHz (system 1) and 110 MHz (system 2). The modulation depth is equal to 400 kHz, i.e. a modulation index of 5. As the central frequency of the probe beam differs from that of the pump beam, the locking position is translated by half of the offset (i.e., 40 and 55 MHz). Since the carrier frequency of an AOM can be tuned up to about 20% of its central value, the locked frequency can be tuned to accommodate the arm-locking requirements. Similar AOMs have already been space qualified for Pharao mission [20], another alternative would be to use the AOMs from LISA Pathfinder, also already space qualified with slightly different technologies [21].

By four waves mixing [22], the modulation is transferred to the probe beam. The carrier sideband interference produces a beat on the probe beam whose amplitude is roughly proportional to the derivative of the line profile and can then be used as an error signal for the feedback electronics. One of the main advantages of the MTS technique is that it is insensitive, at first order, to the residual amplitude noise of the pump (as long as it saturates the molecules) that could be induced by the modulation process. However, we found that the efficiency of the AOMs could change widely, correlated with room temperature, at a level such that the saturation is no longer steady. Consequently, we decided to actively control the pump power by regulating the radio frequency (RF) power fed to the AOM. With this

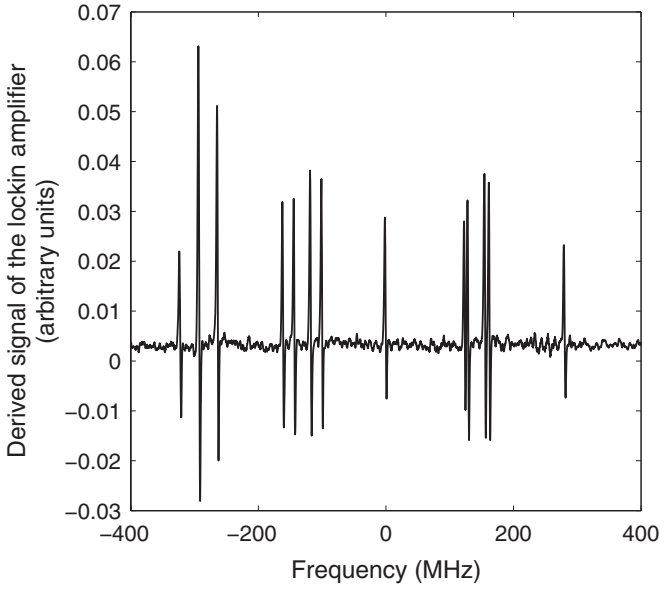

FIG. 3. Rough measurement of the I_2 hyperfine transitions of the R(56)32-0 line from a_2 to a_{15} centered at a_{10}.

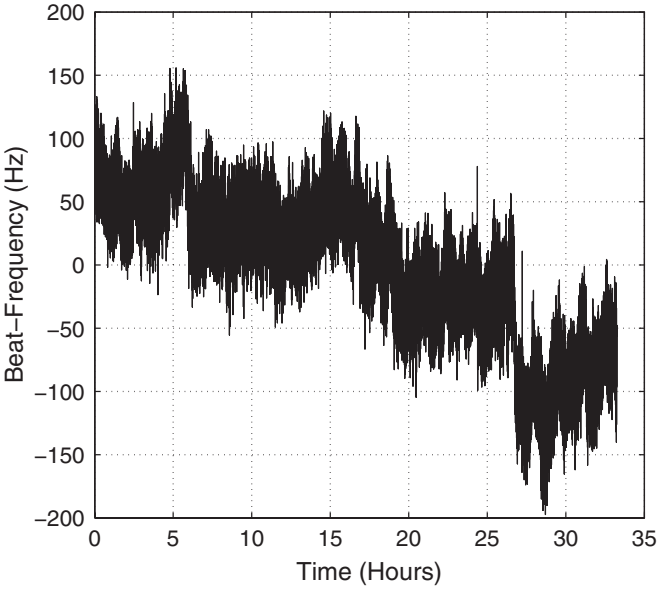

FIG. 4. Time evolution of the beat frequency.

control, the relative stability of power is about 10^{-5} at low frequency (below a few hundred Hertz).

We chose to lock on the a_{10} R(56)32-0 line, which is intrinsically narrow, strong, and sufficiently isolated from other lines. This transition has often been used as a frequency reference and provides very good frequency-stability results over the long time scale, especially beyond 100 s [7–9]. And as can be seen on Fig. 3, its identification is easy even with a free running (i.e., not stabilized) laser. The line width (full width at half maximum of a Lorentzian) is measured at about 800 ± 40 kHz.

The iodine cells have been provided by the Bureau International des Poids et Mesures (BIPM). They are 20 cm long, 25 mm in diameter. Each beam is folded three times in the cell, increasing the effective interaction length to 60 cm. The cold finger of the cells is thermally stabilized at around $-15 \pm 1 \pm 0.01$ °C in order to control the pressure inside the cell that itself affects the line width of iodine. A low pressure induces low absorption (hence low signal and signal-to-noise ratio) whereas high pressure broadens the line and decreases the stability. The iodine pressure is then regulated at $0.82 \pm 0.09 \pm 0.001$ Pa.

After demodulation with a lock-in amplifier, the error signal is fed through the feedback electronics, acting on the temperature and piezoelectric actuator of the laser crystal. The temperature is used for correction on long time scales (below about 70 mHz), whereas the piezoelectric actuator handles higher frequencies, up to about 1 kHz.

IV. RESULTS

A. Frequency stability

Figure 4 shows a typical evolution of the beat frequency when both lasers are locked on the R(56)32-0: a_{10} transition. The frequency drift on 1064 nm is about 200 Hz over more than 30 hours once the systems have had time to stabilize.

Assuming that the two stabilization setups are independent and have the same performance, the power spectrum of the infrared beat is twice the power spectrum of one system: the variance of two independent systems is equal to the sum of the variance of each system. To calculate the power spectrum, we used the pwelch function of MATLAB based on Welch's method which allows averaging the periodogram, a reduction of the noise in the estimated power spectra in exchange of reducing the frequency resolution. The temporal data are first resampled with a step corresponding to the average of the difference between two successive samples (~ 1.2 s). The signal is split into segments of equal length, a periodogram is calculated for each segment, and an averaging of these periodograms is achieved. The estimated linear spectral density for a single laser is plotted in Fig. 5. The solid line corresponds to the laser stability requirements fixed for the LISA mission and therefore our objectives of frequency stability. Thus the frequency noise in terms of linear spectral density has to be below $30 \cdot \sqrt{1 + (\frac{3\ \mathrm{mHz}}{f})^4}\ \mathrm{Hz}/\sqrt{\mathrm{Hz}}$ between 10^{-4} and 1 Hz.

The improvements over our previous system [23] are mainly due to three factors: better temperature stability of the doubling crystals, more precise alignment of the counterpropagating beams into the cell, and a power control of the pump beams.

Above 10 mHz, the spectrum is roughly flat, below our objective of 30 $\mathrm{Hz}/\sqrt{\mathrm{Hz}}$, with a slight tendency to decrease toward 10 $\mathrm{Hz}/\sqrt{\mathrm{Hz}}$ at higher frequencies. Below 10 mHz, the frequency noise rises as $1/f^{\beta}$ with $\beta \simeq 0.9$, which is relatively close to the frequency random walk

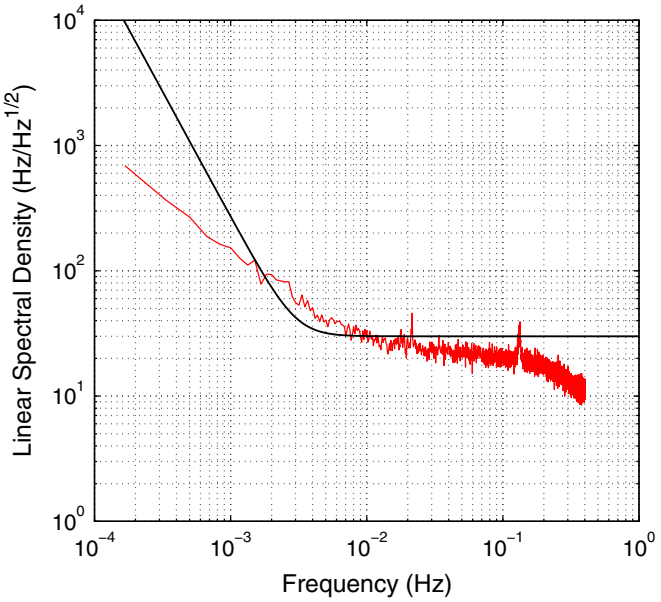

FIG. 5 (color online). Frequency stability of one system. The data used to calculate this linear spectral density are those presented in Fig. 4. The solid curve corresponds to our objective (see text for details).

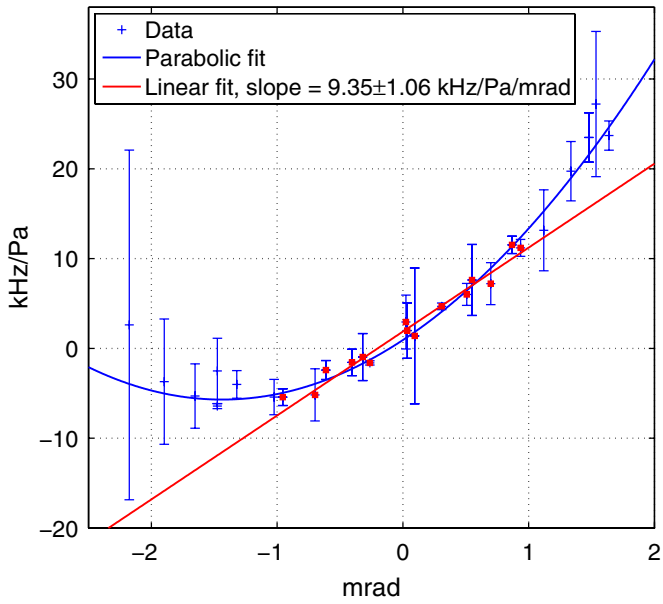

FIG. 6 (color online). Frequency shift induced by temperature fluctuations of the cold finger of the cell versus the angle between the pump and the probe beams. The zero angle corresponds to the ideal counterpropagation of the beams. The upper (blue) curve corresponds to a parabolic fit on all data and the lower (red) curve to a linear fit on data included in the ± 1 mrad interval.

($\beta = 1$). The presence of peaks near to 20 and 140 mHz is not yet really explained. The first, at 20 mHz, seems to be correlated with fluctuations of the room temperature, but we do not have any explanation for the second for the moment. Furthermore, these peaks are not always present for similar experimental conditions. They can shift to slightly different frequencies or even disappear.

B. Frequency shifts and offsets

We measured the frequency shift induced by temperature fluctuations of the cold finger of the cells. We found a strong correlation between the frequency shift and the angle between the probe and the pump beams. This may be linked to the pressure dependence of the asymmetry of the line shape induced by wave front curvature as explained in [26]. Figure 6 shows the evolution of the frequency shift induced by pression fluctuations versus the angle pump/probe. For an ideal overlapping of the two beams, the frequency shift induced by pressure fluctuations is of the order of 1.8 kHz/Pa. This value is consistent with other experiments (see Table I) but the sign is opposite. At ± 1 mrad of the ideal overlapping position, the variation of this coefficient versus the angle can be approximated by a linear fit with a slope of 9.35 ± 1.06 (2-σ systematic deviation) kHz/(Pa mrad). Considering all the data, a parabolic fit is more appropriate; the fitted values are 3.21 ± 0.49 kHz/(Pa mrad^2), 9.22 ± 0.50 kHz/(Pa mrad), and 0.93 ± 0.60 kHz/Pa respectively for a, b, and c coefficients of the equation $ax^2 + bx + c$.

We also measured the frequency shift versus the angle between the two counterpropagating beams at constant pressure. We find a slope of about -20 kHz/mrad. This shift may be correlated with the line dissymmetry when the two beams are not perfectly overlapping. Indeed, wave front curvature introduces a shift of the center and a profile asymmetry of the line shape [26]. Moreover, an angular dependence of intensity and line shape of phase-conjugate emission in theory of degenerate four-wave mixing have already been demonstrated [27].

Another interesting frequency shift is the one induced by pump power fluctuations. We find a slope of about -1.7 kHz/mW, that can be compared to those obtained by the three previous experiments (see third column, Table I). As explained in [7] and [24], the value and sign of the slope is probably linked to beam diameter and wave front curvature.

TABLE I. Frequency shifts due to iodine pressure shift (column 2) and pump power shift (column 3) for this work and similar experiments (column 1).

	Frequency shifts induced by	
	Iodine pressure shift (kHz/Pa)	Pump power shift (kHz/mW)
Reference [24]	-1.3	-2.1
Reference [7]	-3.2	-2
Reference [25]	-2.7	<0.22
This work	1.8	-1.7

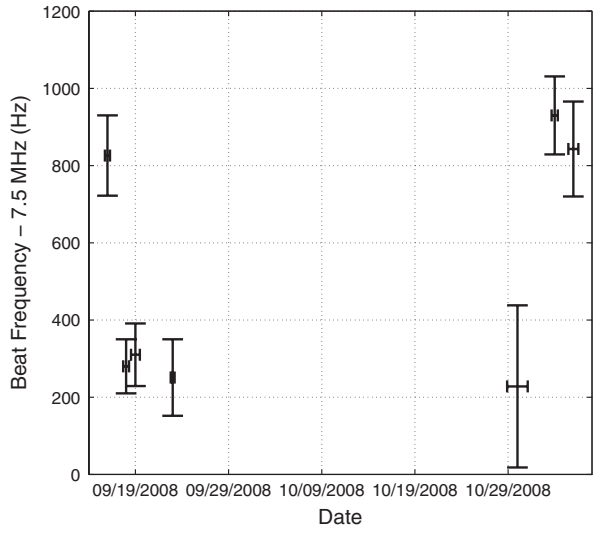

FIG. 7. Evolution of the mean frequency beat. Y-error bars correspond to the standard deviation of the beat frequency measurement and X-error bars to the acquisition period (between half a day and two days).

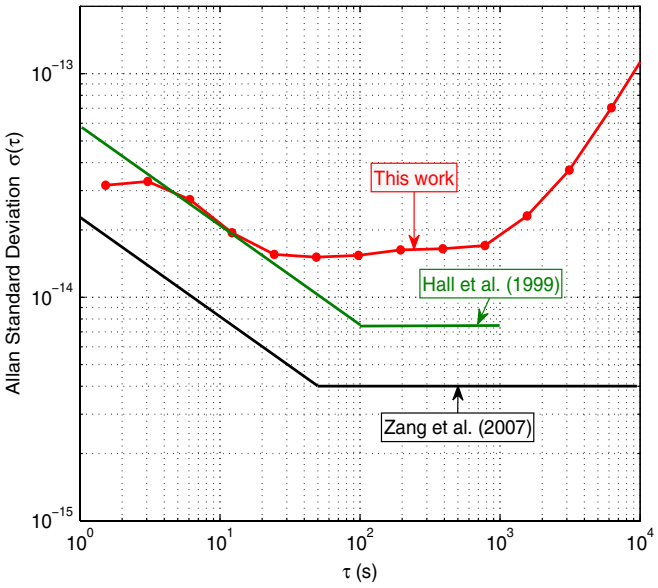

FIG. 8 (color online). Allan standard deviation of our system compared to those obtained by Hall *et al.* [7] and Zang *et al.* [25].

We also tested the reproducibility of the experiment; the results can be seen in Fig. 7. For the same experimental conditions, the mean beat frequency changes less than 600 Hz over a period exceeding one month. And the frequency offset between the two lasers is below 1 kHz, when the same adjustments were made on both systems. As already seen in [24]'s experiment, a systematic offset still exists, maybe due to different wave front curvatures inside the cell for the two systems and systematic effects (offsets) in electronics.

C. Comparison with other experiments

Until recently, Hall and his colleagues held, to our knowledge, the best frequency stability results using iodine molecules at 532 nm (see [7] and [24]). The first main difference with our system is the cell length: they used a single pass 1.2 m long cell. The second is the presence of two active components to drive the frequency and the phase of the pump beam. An AOM was used to frequency shift the pump beam and an electro-optic modulator (EOM) to modulate the phase.

Another interesting experiment is the one of [25]. They hold the best global results in terms of frequency stability using iodine in the 10^{-4}–1 Hz frequency range. As in the Hall experiment, they use an AOM to frequency shift the pump beam and an EOM to phase modulate. They also introduced an active temperature feedback control of the residual amplitude modulation of the EOM. The cell used is 45 cm long that, with four passes inside, increases the interaction length up to 1.8 m.

To compare our stability to those obtained by [7] and [25], we used the Allan standard deviation. The Allan deviation is defined as the square root of the Allan variance given in the following equation:

$$\sigma_y^2(\tau) = \frac{1}{2}\langle(\bar{y}_{n+1} - \bar{y}_n)^2\rangle,$$

where $\bar{y}_n$ is the average normalized frequency deviations taken over the sample period n and τ the duration per sample period. Figure 8 represents the Allan standard deviation of our measurement compared to those obtained by the two other experiments, [7] and [25].

The data show a 3×10^{-14} stability at 1 s. Between a few seconds and about 20 s, the results follow a slope of $\tau^{-1/2}$, where τ is the averaging time. This corresponds to a white frequency noise. From 20 s to about 800 s, the Allan deviation is relatively flat with a value of about 1.5×10^{-14}. Beyond 800 –1000 s, the stability decreases following a slope very close to τ, probably corresponding to a frequency random walk (as the slope of $1/f$ in linear spectral density).

We get similar results of stability to [7] between 1 s and about 20 s. Our results are even better on the short time scales (below some seconds). However, after 20 s, [7]'s stability keeps improving until 100 s before reaching a plateau. They obtain a 7×10^{-15} stability between 100 and 1000 s which is twice as good as the stability of our plateau.

The stability results of [25] are even better. For the short time scales, they obtain a 2.3×10^{-14} stability at 1 s. Then, as for [7] and our experiment, the stability follows $\tau^{-1/2}$ slope, but from 50 s, when the plateau is reached, the stability is around 4×10^{-15} until 10^4 s. Tests with no temperature feedback of the EOM show that the stability begins to decrease from 100 s to reach 2×10^{-14} stability

at 10^4 s. Without the use of this active feedback loop to control the residual amplitude modulation (RAM), the frequency shift induced by the EOM is about -1.2 kHz/K. By comparison, the AOMs are much less sensitive to room temperature fluctuations. In our experiment, changing the temperature of the AOM does not show significant effect on the frequency stability as long as the pump power is stabilized. It is difficult to exactly know the temperature of the crystal, but the frequency shift induced by heating the box of the AOM is in order of 50 Hz/K.

However, we sometimes noticed a strong correlation of the laser stability with room temperature, in order of a few kHz/K. This correlation is still misunderstood; its origin remains under investigation.

V. CONCLUSION

We realized a simple, compact and efficient frequency-stabilized system based on the lock on a molecular transition of iodine. This experiment was not designed to compete with the best stability results obtained in metrology but to be compatible with space requirements. Contrary to previous experiments, we use an acousto-optic modulator for both frequency shifting and modulating the pump beam. The iodine cell is only 20 cm long and that constrains the interaction length to 60 cm (three passes). These choices have been made to keep the system as simple as possible for space applications. All the components, except the iodine cell and the doubling crystals, have already been space qualified and the size of the system 1.1×1.1 m^2 can be further reduced.

We obtained good results, except for long time scales where we are certainly limited by the thermal environment. The forthcoming move to a temperature-stabilized clean room should improve our stability performance in this frequency range. However, these results are already compatible with the LISA frequency-stability requirements and although our primary goal was to develop a simple and robust experiment, our results are comparable to those obtained in metrology and are promising for space application.

ACKNOWLEDGMENTS

The authors thank A. Brillet from the Observatoire de la Côte d'Azur and O. Acef from the Observatoire de Paris for helpful discussions and involvement. We acknowledge the French Space Agency (C.N.E.S.) for technical and financial support of this work, and especially J. Berthon and L. Mondin for their encouragement.

[1] K. Danzmann, Adv. Space Res. **25**, 1129 (2000).
[2] M. Tinto, D. A. Shaddock, J. Sylvestre, and J. W. Armstrong, Phys. Rev. D **67**, 122003 (2003).
[3] B. S. Sheard, M. B. Gray, D. E. McClelland, and D. A. Shaddock, Phys. Lett. A **320**, 9 (2003).
[4] J. Sylvestre, Phys. Rev. D **70**, 102002 (2004).
[5] M. Tinto and M. Rakhmanov, arXiv:gr-qc/0408076.
[6] N. Jedrich, W. Klipstein, J. Livas, P. Maghami, S. Merkowitz, M. Sallusti, D. Shaddock, S. Vitale, W. Weber, and J. Ziemer, ''*LISA Technology Status Report*,'' ESA-NASA, 2006 (unpublished).
[7] J. L. Hall, L.-S. Ma, M. Taubman, B. Tiemann, F. Hong, O. Pfister, and J. Ye, IEEE Trans. Instrum. Meas. **48**, 583 (1999).
[8] S. Picard, L. Robertsson, L.-S. Ma, Y. Millerioux, P. Juncar, J.-P. Wallerand, P. Balling, P. Kren, K. Nyholm, M. Merimaa, T. Ahola, and F.-L. Hong, IEEE Trans. Instrum. Meas. **52**, 236 (2003).
[9] J. Ye, L. Robertsson, S. Picard, M. Long-Sheng, and J. Hall, IEEE Trans. Instrum. Meas. **48**, 544 (1999).
[10] J. C. Livas, J. I. Thorpe, K. Numata, S. Mitryk, G. Mueller, and V. Wand, Classical Quantum Gravity **26**, 094016 (2009).
[11] P. W. McNamara, H. Ward, and J. Hough, Adv. Space Res. **25**, 1137 (2000).
[12] V. Leonhardt and J. B. Camp, in *Proceedings of the Sixth Edoardo AMALDI Conference on Gravitational Waves, Okinawa, Japan, 2005*, http://tamago.mtk.nao.ac.jp/amaldi6/poster.html.
[13] K. McKenzie, R. E. Spero, and D. A. Shaddock, Phys. Rev. D **80**, 102003 (2009).
[14] S. Picard, L. Robertsson, L. Ma, K. Nyholm, M. Merimaa, T. E. Ahola, P. Balling, P. Kren, and J.-P. Wallerand, Appl. Opt. **42**, 1019 (2003).
[15] L. Mondin, Ph.D. thesis, Université de Nice-Sophia Antipolis, 2005.
[16] M. Tröbs, S. Barke, J. Mbius, M. Engelbrecht, D. Kracht, L. d'Arcio, G. Heinzel, and K. Danzmann, J. Phys. Conf. Ser. **154**, 012016 (2009).
[17] R. Stebbins *et al.*, ''Laser Interferometer Space Antenna (LISA), Space Response,'' Astro2010 RFI #2 2009, http://lisa.gsfc.nasa.gov/Documentation/Astro2010_RFI2_LISA.pdf.
[18] V. Leonhardt and J. B. Camp, Appl. Opt. **45**, 4142 (2006).
[19] W. Demtroder, in *Laser Spectroscopy*, edited by S.-V. B. Heidelberg (Springer-Verlag, Berlin, 2003), 3rd ed..
[20] P. Lemonde (private communication).
[21] P. Prat (private communication).
[22] R. K. Raj, D. Bloch, J. J. Snyder, G. Camy, and M. Ducloy, Phys. Rev. Lett. **44**, 1251 (1980).
[23] H. Halloin, O. Acef, B. Argence, O. Jeannin, P. Prat, O. Turazza, E. de Vismes, G. Auger, E. Plagnol, A. Brillet, L. Mondin, and J. Berthon, in *International Conference on*

Space Optics, Toulouse, France, 2008, http://www.icsoconference2008.com/cd/page_30sessions.pdf.
[24] M. L. Eickhoff and J. L. Hall, IEEE Trans. Instrum. Meas. **44**, 155 (1995).
[25] E. J. Zang, J. P. Cao, Y. Li, C. Y. Li, Y. K. Deng, and C. Q. Gao, IEEE Trans. Instrum. Meas. **56**, 673 (2007).
[26] C. J. Bordé, J. L. Hall, C. V. Kunasz, and D. G. Hummer, Phys. Rev. A **14**, 236 (1976).
[27] M. Ducloy and D. Bloch, J. Phys. (Paris) **42**, 711 (1981).